Impacts of information flow topology on traffic dynamics of CAV-MV heterogeneous flow

Tiancheng Ruan, Hao Wang, Linjie Zhou, Yantang Zhang, Changyin Dong, Zewen Zuo,

***Abstract*—With the development of Connected Autonomous Vehicle (CAV) technology, different information flow topologies (IFTs) have been applied to CAV Ad Hoc Networks. Firstly, from the perspective of the controller, a general model is proposed to directly reflect the actual communication effect on the controller instead of simply abstracting it into the optimal time interval, which is more feasible. Secondly, linear stability analysis is carried out based on the general model where different time delays are considered, and stability criterion is obtained for subsequent analysis. Thirdly, for the Predecessor-Leader Following (PLF), one of the three IFTs, the optimal parameter configuration is obtained. Finally, we compare the three main IFTs through numerical simulation and analyze the difference in stability region, robustness, safety, and emission between platoon Cooperative Adaptive Cruise Control (CACC) controllers based on different IFTs. It is found that the CACC platoon controller based on PLF can maintain a similar margin desire time gap in the whole velocity range while a traditional one cannot, which means a significant gain of traffic capacity and safety via communication. Besides, among the three IFTs, PLF is the most suitable one as the IFT used by CACC can bring significant capacity gains while occupying a smaller communication bandwidth.**

***Index Terms*—Connected and Automated Vehicles (CAVs); CAV platoon; linear stability; platoon management; information topology flow(IFT).**

I. Introduction

WITH the rapid development of transportation systems, to maintain traffic safety, mobility, and environmental sustainability, Connected Autonomous Vehicle (CAV) technology has attracted increasing attention and developed rapidly over the past decade. The level of connectivity and automation in vehicles have improved dramatically. Vehicle-to-infrastructure (V2I) communications enable partial or complete autonomous driving with onboard sensors, and vehicle-to-vehicle (V2V) communications enable collaboration and communication between vehicles.[1]

The most typical application of V2V communication is Cooperative Adaptive Cruise Control (CACC). A vehicle controlled by this system automatically maintains a constant time gap with the preceding vehicle. Simulation results and field experiments reveal that CACC-enabled vehicles can maintain a shorter time gap compared with manual vehicles. Therefore, consecutive CACC-enabled vehicles can form a string-based driving mode through V2V communication to improve traffic efficiency.[2][3]

A CAV string consists of a leader vehicle and several following vehicles, which maintain a smaller constant time gap. The formation of CAVs string mainly depends on the workshop communication protocol and the roadside unit communication protocol. The CAV string can break through the limitations of vehicle communication and control and improve traffic efficiency and safety by obtaining more surrounding information in time.[4]

Cellular vehicle-to-everything (C-V2X) has been selected as the standard communication protocol for CAVs. However, due to the limitations of C-V2X communication, a CAV string cannot be extended indefinitely, which means that a CAV string is divided into several CAV platoons. The CAV platoon, the subject of this paper, consists of a leader vehicle degraded to Adaptive Cruise Control (ACC) due to loss of communication gain and several CAVs within communication range.

At present, there has been a lot of research on CACC string stability. Some studies conducted linear stability analysis of CACC string stability using PATH-CACC and Intelligent Driver Model (IDM) as microscopic longitudinal control models.[5][6] Other studies incorporated assisted strategies for communicating information, such as Connected Cruise Control (CCC) into the framework of linear stability analysis.[7][8]

In general, most current theoretical studies did not precisely reflect the communication function of CACC in the longitudinal control model but calculated the capacity gain brought by it, which is sufficient to simulate the longitudinal behavior of CACC but not suitable for controller design. Furthermore, CACC communication is usually based on Vehicular Mobile Ad Hoc Networks (VANETs), which means communication is based on a specific information flow topology (IFT) in practical application. For the above reasons, the CACC longitudinal control model should also be designed based on a specific IFT, which is ignored by existing researches.[9][10][11]

To fill the gap in this field, this paper takes platoon management and direct information (obtained via communication) into consideration. Firstly, we delivered an extended model considering different IFTs. Secondly, the linear stability analysis was performed to obtain the string stability criterion for the CACC platoon based on the extended model. Thirdly, we explored the stability region at different velocitys and parameters of the CACC platoon. Finally, the numerical analyses were conducted to determine the difference in stability, robustness,

T. Ruan, H. Wang, L. Zhou, C. Dong and Z. Zuo are with the School of Transportation, Southeast University, Nanjing 211189, P.R. China; Jiangsu Key Laboratory of Urban ITS, Southeast University, Nanjing, 210096, P.R. China; Jiangsu Province Collaborative Innovation Center of Modern Urban Traffic Technologies, Southeast University, Nanjing, 210096, P.R. China(e-mail: ruantiancheng@seu.edu.cn; haowang@seu.edu.cn; 220193107@seu.edu.cn; dongcy@seu.edu.cn; 220203312@seu.edu.cn).

Y. Zhang is with School of Transportation Science and Engineering, Harbin Institute of Technology, Harbin, 150090, China(e-mail: 19S132063@stu.hit.edu.cn).

Manuscript received July 1, 2021.(Corresponding author: Hao Wang.)

safety, and emission of different IFTs. The paper ended with brief concluding remarks and a discussion of future work.

The layout of the paper is the following. In Section II, the typical IFTs and the composition of CACC platoon are introduced; In Section III, we propose a general model to simulate CACC longitudinal control and multiple time delays of different vehicles; In Section IV, the linear characteristic equation analytical method is implemented to obtain the string stability criterion of the CACC platoon controller under multiple time delays; In Section V, numerical analyses are used to verify the theoretical analysis results from the perspective of long-wave and short-wave stability, and the differences in stability, robustness, safety, and emission of different IFTs have been explored; In Section VI, main contributions and achievements of this paper are summarized.

II. Analytical expression of heterogeneous traffic flow

A. Typical information flow topologies

The communication module of a CACC system facilitates real-time and reliable wireless V2V/I2V communication, which can not only provide additional information that cannot be readily detected by perception sensors, but also in a quicker and more accurate manner.

The information flow topology (IFT) defines the starting point, terminal point, and the corresponding communication pattern of the CACC, which significantly impacts the effectiveness and efficiency of communication.[12] The three representative IFTs of CACC are shown in Fig. 1. The most commonly used topology is the predecessor following (PF) where the following vehicle only receives the communication signal from its predecessor. However, the inability of PF to obtain information from distant vehicles makes it unable to make full use of the advantages of communication. In response to this feature, predecessor-leader following (PLF) is proposed. Using PLF enables CACC to receive the information from the platoon leader, which means perceiving the traffic conditions far ahead to respond in advance to improve the stability of the traffic flow. The IFT that further leverages the communication ability of CACC is multiple-predecessor-leader-following (MPLF).[13][14] By utilizing the information of all preceding vehicles in the platoon, the following vehicle can better maintain the stability of the traffic flow.

B. Traffic Flow Configurations

As shown in Fig. 2, platoon management is expressed under the condition that when the CACC string reaches the maximum number of vehicles that C-V2X can maintain stable communication, the existing platoon is not included in the subsequent CACC, but a newly-formed platoon. The platoon size S is limited by the maximum C-V2X communication bandwidth. Assume that the traffic flow includes three types of vehicles:

1) *MV* (Manual Vehicle) - regular cars maneuvered by humans;
2) *LV* (Leader Vehicle) - the leader vehicle of the platoon following an MV and its control mechanism is similar to ACC, which cannot obtain the gain of communication and only sends information to its following vehicles;[15]
3) *PV* (Platoon Vehicle) - the vehicle inside the platoon which receives information from both preceding vehicle and platoon leader vehicle; The information flow topology of this type of vehicle can be Predecessor-Following (PF), Predecessor-Leader Following (PLF), or multiple-predecessor-leader-following (MPLF). [15].

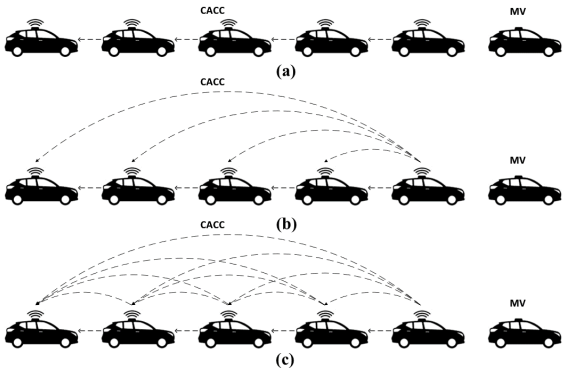

Fig. 1: Typical information flow topologies: (a) predecessor-following (PF), (b) predecessor-leader-following (PLF), (c) multiple-predecessor-leader-following (MPLF).

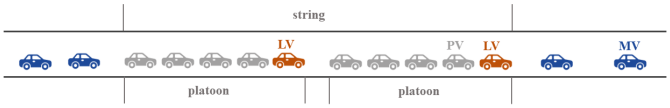

Fig. 2: The Traffic Flow Configurations.

This paper mainly analyzes the linear string stability of CACC platoon and designs controller under different IFTs. The specific platoon consists of a LV and $S-1$ PVs.

III. Car-Following Model

A. Car-Following Model

In previous studies, there are generally two methods for modeling the car-following behavior of CACC: 1) simulating based on modified traffic flow models,[16][17][18] and 2) modeling based on vehicle models or controllers with experimental data.[19][20][21] From the practical application perspective, there is no doubt that the data model based on field tests is closer to the actual situation. However, the high cost and safety risks of CACC field trials make it impractical to conduct large-scale field trials at present. Furthermore, using the data model to model the longitudinal behavior abstracts the internal mechanism of the controller, which is not conducive to the design of the CACC controller. In summary, this paper is mainly based on simulations instead of field tests. Moreover, a general form is used to simulate longitudinal car-following for the sake of universality and suitability.

1) ACC Model: As for ACC, due to the lack of communication modules, the car-following decision is completely based on its perception of the surrounding situation. According to the existing models used to describe the ACC car-following

behavior, its decision-making mainly depends on its velocity, the space headway from the preceding vehicle, and the velocity difference with the preceding vehicle. Therefore, the general form used in this article is as follows:

$$\frac{dv_n(t)}{dt} = g_n\left(v_n(t-\tau), s_n(t-\tau), \Delta v_n(t-\tau)\right), \tag{1}$$

where $g_n(t)$ is the acceleration; τ is the time delay of decision; $v_n(t)$ is the velocity; $\Delta v_n(t)$ is the velocity difference between the subject vehicle and the preceding vehicle; $s_n(t)$ is the space headway between the subject vehicle and its predecessor.

2) CACC Model: The CACC system, which incorporates a V2V communication module, is an enhancement of the ACC system. With the gain of communication for system stability, CACC can maintain smaller time gap and perception delay, thereby improving traffic capacity and safety. According to the definition of CACC[22], the essential component is the communication module, which receives information from other CACC-enabled vehicles through VANET. Instead of simply using a smaller time gap to represent communication gain, an additional component has been added to the longitudinal model to describe the communication gain which represents the information obtained from preceding vehicles via the communication module.

For PF, the transmitted information only includes the position, velocity, and acceleration of the preceding vehicle, so the general form used to simulate CACCs based on PF is as follows:

$$\begin{aligned}\frac{dv_n(t)}{dt} =& g_n\left(v_n(t-\tau), s_n(t-\tau), \Delta v_n(t-\tau)\right) \\ &+ \gamma_p g_{n-1}\left(v_{n-1}(t-\tau), s_{n-1}(t-\tau), \Delta v_{n-1}(t-\tau)\right),\end{aligned} \tag{2}$$

where $g_n(*)$ the acceleration based on the general form of ACC system; γ_p is the weighting coefficient of communication gain from the preceding vehicle.

As for PLF, the transmitted information includes the position, velocity, and acceleration of the platoon leader vehicle and preceding vehicle. In this case, the general form used to simulate CACCs based on PLF is as follows:

$$\begin{aligned}\frac{dv_n(t)}{dt} =& g_n\left(v_n(t-\tau), s_n(t-\tau), \Delta v_n(t-\tau)\right) \\ &+ \gamma_p g_{n-1}\left(v_{n-1}(t-\tau), s_{n-1}(t-\tau), \Delta v_{n-1}(t-\tau)\right) \\ &+ \gamma_l g_1\left(v_1(t-\tau), s_1(t-\tau), \Delta v_1(t-\tau)\right),\end{aligned} \tag{3}$$

where, γ_p is the weighting coefficient of communication gain from preceding vehicle; γ_l is the weighting coefficient of communication gain from leader vehicle.

When the problem comes to MPLF, the transmitted information included the position, velocity, and acceleration of the platoon leader and all the preceding vehicles in the platoon. Therefore, the expression of the general form for CACC based on MPLF is as follows

$$\begin{aligned}\frac{dv_n(t)}{dt} =& g_n\left(v_n(t-\tau), s_n(t-\tau), \Delta v_n(t-\tau)\right) \\ &+ \sum_{k=1}^{n-1} \gamma_k g_{n-k}\left(v_{n-k}(t-\tau), s_{n-k}(t-\tau), \Delta v_{n-k}(t-\tau)\right),\end{aligned} \tag{4}$$

where $\gamma_1 = \gamma_2 = \cdots = \gamma_{n-1}$ represent the information communicated from leader and preceding vehicle has identical importance.

B. Reaction delay composition

Different types of vehicles have various reaction delays in the process of perceiving the surrounding environment[23][24]. It is worth noting that reaction delays in this paper refers to the delays of perception. Based on existing research and difference of perceived variables, we can divide the reaction delay into two parts: the reaction delay to the car-following gap τ_n^s , and the reaction delay to the velocity difference $\tau_n^{\Delta v}$, where the reaction delay to vehicle velocity is due to the driver's focusing on the velocity of vehicle all the time.

1) *MVs*: Since the reaction performance of MVs cannot benefit from the intelligent and connected environment during driving, their time delays do not change. Set the time delay value to: τ_{mv}^s=0.4s, $\tau_{mv}^{\Delta v}$=0.4s;
2) *LVs*: Since LVs are controlled by the Adaptive Cruise Control system, there is no response time delay and decision time delay. However, it cannot communicate, and sensing the state of the vehicle ahead depends entirely on the onboard radar, which has an inevitable sensing delay. Set the delay value to: τ_{lv}^s=0.2s, $\tau_{lv}^{\Delta v}$=0.2s;
3) *PVs*: Due to the intelligent and connected environment, PVs receive the information of the vehicle ahead through the onboard communication system, so its communication delay is almost negligible compared with other delays. Set the delay value to: τ_{pv}^s=0s, $\tau_{pv}^{\Delta v}$=0s.

IV. Linear Stability analysis of CACC platoon controller

In this section, since most of the disturbances faced by drivers during normal driving are small disturbances, we apply the linear stability method for the extended intelligent driver model described by Equation(2)-(4) to obtain the stability criterion of the CACC platoon.[25][26] Since CACCs based on different IFTs use a similar general model, they can apply the framework of linear stability analysis to obtain the corresponding stability criteria in a similar process. Hence, the following content only takes CACC based on PLF as an example. In the equilibrium state, the vehicle velocity in the traffic flow is equal to the equilibrium state velocity v_e; the velocity difference between adjacent vehicles is zero; the car-following gap between the vehicles maintains the desired gap s_n^e; and the acceleration of the vehicle is zero. So, we can get:

$$\begin{cases} v_n = v_n^e, \\ s_n = s_n^e, \\ \Delta v_n = 0, \\ g_n\left(v_n^e, s_n^e, 0\right) = 0. \end{cases} \tag{5}$$

Now let δv_n and δs_n denote the small deviation of the velocity and gap around the equilibrium state. The state after the disturbance can be expressed as:

$$\begin{cases} v_n = v_n^e + \delta v_n, \\ s_n = s_n^e + \delta s_n, \\ \Delta v_n = 0 + \Delta(\delta v_n). \end{cases} \tag{6}$$

By introducing the multiple reaction delays into the:

$$\begin{aligned} \frac{d\delta v_n(t)}{dt} &= g_n\left(v_n^e, s_n^e, 0\right) + g_n\left(v_n(t), s_n\left(t-\tau_n^s\right), \Delta v_n\left(t-\tau_n^{\Delta v}\right)\right) \\ &+ \gamma_p g_{n-1}\left(v_{n-1}(t), s_{n-1}\left(t-\tau_{n-1}^v\right), \Delta v_{n-1}\left(t-\tau_{n-1}^v\right)\right) \\ &+ \gamma_l g_1\left(v_1(t), s_1\left(t-\tau_1^v\right), \Delta v_1\left(t-\tau_1^v\right)\right). \end{aligned} \tag{7}$$

Substituting equation (5) and (6) into (7), the acceleration expression under small disturbance is as follows:

$$\begin{aligned} \frac{d\delta v_n(t)}{dt} &= g_n^v \delta v_n(t) + g_n^s \delta s_n\left(t-\tau_n^s\right) - g_n^{\Delta v}\Delta\left(\delta v_n\left(t-\tau_n^{\Delta v}\right)\right) \\ &+ \gamma_p\left[g_{n-1}^v \delta v_{n-1}(t) + g_{n-1}^s \delta s_{n-1}\left(t-\tau_{n-1}^s\right)\right. \\ &\left.- g_{n-1}^{\Delta v}\Delta\left(\delta v_{n-1}\left(t-\tau_{n-1}^{\Delta v}\right)\right)\right] \\ &+ \gamma_l\left[g_1^v \delta v_1(t) + g_1^s \delta s_1\left(t-\tau_1^s\right) - g_1^{\Delta v}\Delta\left(\delta v_1\left(t-\tau_1^{\Delta v}\right)\right)\right], \end{aligned} \tag{8}$$

$$\frac{d\delta s_n(t)}{dt} = \delta v_{n-1}(t) - \delta v_n(t), \tag{9}$$

where $g_n^v = \left.\frac{\partial g_n}{\partial v_n}\right|_{(v_n^e, s_n^e, 0)}, g_n^s = \left.\frac{\partial g_n}{\partial s_n}\right|_{(v_n^e, s_n^e, 0)}, g_n^{\Delta v} = \left.\frac{\partial g_n}{\partial \Delta v_n}\right|_{(v_n^e, s_n^e, 0)}$ is the partial differential equations for velocity, gap, velocity difference, respectively. To obtain the characteristic equation under the disturbance, a reasonable form hypothesis for the disturbance must be proposed. Considering that the disturbance from the preceding vehicle is not equal to zero, the traditional Fourier-ansatz $\delta v_n(t) = \hat{v}e^{\lambda t}$ and $\delta s_n(t) = \hat{s}e^{\lambda t}$ are not applicable. Based on the superposition principle of linear system, Fourier-ansatz can evolve into $\delta v_n(t) = \hat{\mathrm{v}}e^{in\varphi+\lambda t}$ and $\delta s_n(t) = \hat{\mathrm{s}}e^{in\varphi+\lambda t}$ to represent the disturbance from the preceding vehicle, where $\hat{\mathrm{v}}$ and $\hat{\mathrm{s}}$ are constants independent of n and t. Based on the Fourier-ansatz and difference equation (9), we can obtain:

$$s_n = \frac{v_{n-1}(t) - v_n(t)}{\lambda}. \tag{10}$$

Take Fourier-ansatz and Equation (10) into (8):

$$\begin{cases} \lambda^2 = \psi_n + \gamma_p \psi_{n-1} e^{-i\varphi} + \gamma_l \psi_1 e^{-i(n-1)\varphi}, \\ \psi_n = g_n^s e^{-\lambda\tau_n^s}\left(e^{-i\varphi} - 1\right) + g_n^v \lambda - g_n^{\Delta v} e^{-\lambda_n^{\Delta v}}\left(e^{-i\varphi} - 1\right)\lambda. \end{cases} \tag{11}$$

The reaction delay term is exponentially expanded to the second order, $e^{-\lambda\tau} = 1 - \lambda\tau + (\lambda\tau)^2/2$, and the third-order characteristic equation of λ is obtained:

$$\psi_n = \left[A_n\lambda^3 + B_n\lambda^2 + C_n\lambda^1 + D_n\lambda^0\right] + \left[H_n\lambda^3 + I_n\lambda^2 + J_n\lambda^1 + K_n\lambda^0\right]e^{-i\varphi}, \tag{12}$$

where,

$$\begin{cases} A_n = 0.5 g_n^{\Delta v}\left(\tau_n^{\Delta v}\right)^2, \\ B_n = -\left(g_n^{\Delta v}\tau_n^{\Delta v} + 0.5 g_n^s\left(\tau_n^s\right)^2\right), \\ C_n = g_n^v + g_n^{\Delta v} + g_n^s \tau_n^s, \\ D_n = -g_n^s, \\ H_n = -0.5 g_n^{\Delta v}\left(\tau_n^{\Delta v}\right)^2, \\ I_n = g_n^{\Delta v}\tau_n^{\Delta v} + 0.5, g_n^s\left(\tau_n^s\right)^2, \\ J_n = -\left(g_n^{\Delta v} + g_n^s \tau_n^s\right), \\ K_n = g_n^s. \end{cases} \tag{13}$$

Substitute Equation (13) into (11), the third-order characteristic equation of CACC platoon is as follows:

$$\begin{aligned} \lambda^2 = &\left[A_n\lambda^3 + B_n\lambda^2 + C_n\lambda^1 + D_n\lambda^0\right] + \left[H_n\lambda^3 + I_n\lambda^2 + J_n\lambda^1 + K_n\lambda^0\right]e^{-i\varphi} \\ &+ \gamma_p\left[A_{n-1}\lambda^3 + B_{n-1}\lambda^2 + C_{n-1}\lambda^1 + D_{n-1}\lambda^0\right]e^{-i\varphi} \\ &+ \gamma_p\left[H_{n-1}\lambda^3 + I_{n-1}\lambda^2 + J_{n-1}\lambda^1 + K_{n-1}\lambda^0\right]e^{-i2\varphi} \\ &+ \gamma_l\left[A_1\lambda^3 + B_1\lambda^2 + C_1\lambda^1 + D_1\lambda^0\right]e^{-i(n-1)\varphi} \\ &+ \gamma_l\left[H_1\lambda^3 + I_1\lambda^2 + J_1\lambda^1 + K_1\lambda^0\right]e^{-in\varphi}. \end{aligned} \tag{14}$$

To maintain linear string stability of CACC platoons, the solutions of the third-order characteristic equation λ satisfies $\mathrm{Re}(\lambda)\leq 0$. The zero solution $\varphi = 0, \lambda_0 = 0$ of the real number domain that satisfies the conditions can be easily obtained. In order to analyze the changing trend of λ with φ. Suppose λ is the power series solution: Among them, λ_1 and λ_2 are real coefficients. At the same time, expand $e^{-i\varphi N}$ to a second-order power series: $e^{-i\varphi N} = 1 - i\varphi N - \frac{N^2\varphi^2}{2}$. By solving the algebraic formula, we can get:

$$\begin{aligned} \Gamma(\varphi) = &\left[C_n + J_n + \gamma_p\left(C_{n-1} + J_{n-1}\right) + \gamma_l\left(C_1 + J_1\right)\right]\lambda_1 \\ &- \left[K_n + \gamma_p\left(D_{n-1} + 2K_{n-1}\right) + \gamma_l\left((n-1)D_1 + nK_1\right)\right] = 0, \end{aligned} \tag{15}$$

$$\begin{aligned} \Gamma\left(\varphi^2\right) = &\left[C_n + J_n + \gamma_p\left(C_{n-1} + J_{n-1}\right) + \gamma_l\left(C_1 + J_1\right)\right]\lambda_2 \\ &- \left[\left(B_n + I_n - 1\right) + \gamma_p\left(B_{n-1} + I_{n-1}\right) + \gamma_l\left(B_1 + I_1\right)\right]\lambda_1^2 \\ &+ \left[J_n + \gamma_p\left(C_{n-1} + 2J_{n-1}\right) + \gamma_l\left((n-1)C_1 + \mathrm{n}J_1\right)\right]\lambda_1 \\ &- \left[0.5K_n + \gamma_p\left(0.5D_{n-1} + 2K_{n-1}\right)\right. \\ &\left. + \gamma_l\left(0.5(n-1)^2 D_1 + 0.5n^2 K_1\right)\right] = 0. \end{aligned} \tag{16}$$

The expression of λ_1 and λ_2 can be obtained by solving the Equation (15) and (16):

$$\begin{aligned} \lambda_1 &= \frac{\left[K_n + \gamma_p\left(D_{n-1} + 2K_{n-1}\right) + \gamma_l\left((n-1)D_1 + nK_1\right)\right]}{\left[C_n + J_n + \gamma_p\left(C_{n-1} + J_{n-1}\right) + \gamma_l\left(C_1 + J_1\right)\right]} \\ &= \frac{g_n^s + \gamma_p g_{n-1}^s + \gamma_l g_1^s}{g_n^v + \gamma_p g_{n-1}^v + \gamma_l g_1^v}, \end{aligned} \tag{17}$$

$$\lambda_2 = \frac{\begin{array}{c}\left[(B_n+I_n-1)+\gamma_p(B_{n-1}+I_{n-1})+\gamma_l(B_1+I_1)\right]\lambda_1^2 \\ -\left[J_n+\gamma_p(C_{n-1}+2J_{n-1})+\gamma_l((n-1)C_1+nJ_1)\right]\lambda_1 \\ +\left[0.5K_n+\gamma_p(0.5D_{n-1}+2K_{n-1})+\gamma_l\left(0.5(n-1)^2D_1+n^2K_1\right)\right]\end{array}}{\left[C_n+J_n+\gamma_p(C_{n-1}+J_{n-1})+\gamma_l(C_1+J_1)\right]}$$

$$\begin{aligned}&-\lambda_1^2+\left[\left(g_n^{\Delta v}+g_n^s\tau_n^s\right)+\gamma_p\left(g_{n-1}^{\Delta v}+g_{n-1}^s\tau_{n-1}^s-g_{n-1}^v\right)\right. \\ &\left.+\gamma_l\left(g_1^{\Delta v}+g_1^s\tau_1^s-(n-1)g_1^v\right)\right]\lambda_1 \\ &=\frac{+\left[0.5g_n^s+\gamma_p 1.5g_{n-1}^s+0.5(2n-1)\gamma_1 g_1^s\right]}{g_n^v+\gamma_p g_{n-1}^v+\gamma_l g_1^v}.\end{aligned} \tag{18}$$

From the conditions of $g_n^s > 0, g_n^v < 0$, it can be known that λ_1 always satisfies the stability condition, then the criterion of string stability becomes $\lambda_2 \le 0$:

$$\begin{aligned}&-\lambda_1^2+\left[\left(g_n^{\Delta v}+g_n^s\tau_n^s\right)+\gamma_p\left(g_{n-1}^{\Delta v}+g_{n-1}^s\tau_{n-1}^s-g_{n-1}^v\right)\right. \\ &\left.+\gamma_l\left(g_1^{\Delta v}+g_1^s\tau_1^s-(n-1)g_1^v\right)\right]\lambda_1 \\ &\frac{+\left[0.5g_n^s+\gamma_p 1.5g_{n-1}^s+0.5(2n-1)\gamma_1 g_1^s\right]}{g_n^v+\gamma_p g_{n-1}^v+\gamma_l g_1^v}\le 0.\end{aligned} \tag{19}$$

For the CACC platoon, $g_n^s = g_{n-1}^s = g_1^s$, $g_n^{\Delta v} = g_{n-1}^{\Delta v} = g_1^{\Delta v}$, $g_n^v = g_{n-1}^v = g_1^v$ should be satisfied, which means Equation (19) can be simplified as:

$$\begin{aligned}F=&-g_n^s+\left[g_n^{\Delta v}\left(1+\gamma_p+\gamma_l\right)+g_n^s\left(\tau_n^s+\gamma_p\tau_{n-1}^s+\gamma_l\tau_1^s\right)+\left(\gamma_p+(n-1)\gamma_l\right)g_n^v\right]g_n^v \\ &+(g_n^v)^2\left[0.5+1.5\gamma_p+0.5(2n-1)\gamma_l\right] \\ &=g_n^v g_n^s\left[\tau_n^s+\gamma_p\tau_{n-1}^s+\gamma_l\tau_1^s\right]+g_n^v g_n^{\Delta v}\left[1+\gamma_p+\gamma_l\right] \\ &+0.5(g_n^v)^2\left[1+\gamma_p+\gamma_l\right]-g_n^s\ge 0.\end{aligned} \tag{20}$$

For the sake of brevity of the article, the specific stability criterion derivation process is omitted. Applying the above similar linear stability analysis method, the corresponding string stability criterions of PF and MPLF are as follows:

$$g_n^v g_n^s\left[\tau_n^s+\gamma_p\tau_{n-1}^s\right]+g_n^v g_n^{\Delta v}\left[1+\gamma_p\right]+0.5(g_n^v)^2\left[1+\gamma_p\right]-g_n^s\ge 0, \tag{21}$$

$$g_n^v g_n^s\left[\tau_n^s+\sum_{k=1}^{n-1}\gamma_k\tau_{n-k}^s\right]+g_n^v g_n^{\Delta v}\left[1+\sum_{k=1}^{n-1}\gamma_k\right]+0.5(g_n^v)^2\left[1+\sum_{k=1}^{n-1}\gamma_k\right]-g_n^s\ge 0. \tag{22}$$

V. Numerical Analyses

Based on the stability criterion of the CACC platoon controller in Equation (20)-(22) obtained in Section IV, this section carries out a numerical analysis on the stability region related to desire time gap and velocity, and a comparison with the traditional ACC controller is conducted. The corresponding simulation verification is carried out under specific parameters. And we explored the difference of stability region under different controller designs for platoon CACCs, including PF-based, PLF-based, and MPLF-based.

TABLE I: Parameters chosen for IDM.

Parameter	A	v_f	δ	s_0	T	b	l
Value	1 m/s^2	33.3 m/s	4	2 m	0.1 – 3 s	2 m/s^2	5 m

To conduct a specific comparative analysis of the differences between different IFTs, a specific model needs to be selected to replace the general form used above. The Intelligent Driver Model (IDM) is chosen for the following reasons. Firstly, the IDM, having only six parameters with concrete meanings, has been proven to precisely model car-following behaviors. Secondly, many studies used the IDM to model ACC and CACC vehicles[27][28], which also indicates the ability of the model to reflect operations of driving-assistant systems. The model is expressed as:

$$g_n(t) = A\left[1-\left(\frac{v_n(t)}{v_f}\right)^\delta-\left(\frac{s_0+T_n v_n(t)+\frac{v_n(t)\Delta v_n(t)}{2\sqrt{Ab}}}{s_n(t)-l_n}\right)^2\right], \tag{23}$$

where $g_n(t)$ is the acceleration; A denotes the maximum desired acceleration; $v_n(t)$ is the velocity; v_f is the free-flow velocity; δ is the acceleration component ($\delta > 0$); s_0 is the minimum safety distance; T_n is the safety time headway; $\Delta v_n(t)$ is the velocity difference between the subject vehicle and the preceding vehicle; b_i is the absolute maximum desired deceleration; $s_n(t)$ is the space headway between the preceding and the subject vehicle; and l_n is the length of the vehicle. The parameters are shown in Table.I,[29][30] which are based on previous studies.

A. stability region of CACC controller

1) Margin stable curves of different IFTs: The basic principle of controller design is that a controller can keep string stable, so it is necessary to compare the margin stable curves of the three IFTs that can keep the string stable to get the margin stable time gap which is directly related to the traffic capacity. From this perspective, we need to obtain the corresponding critical stability conditions for different IFTs.

Assuming the information from the leader and preceding vehicle is of equal importance, the γ_p is set equal to γ_l in this study. In addition, the weighting coefficient of communication gain of different IFTs is all set to 0.3 to make them comparable. Based on the string stability criterion of different IFTs in Equation (20)-(22), the margin stable curves in the space (velocity-desire time gap) are expressed in Fig. 3. When the traffic flow environment is above the margin stable curve, it is string stable at equilibrium state, while the opposite represents the unstable traffic flow.

It can be seen from Fig. 3 that the curve of PF will have a significant unstable peak while the curve of PLF can significantly suppress the appearance of this peak under similar parameter settings to maintain a lower desire time gap in the entire velocity range. In addition, the curve of PLF is significantly lower than the curve of PF, and the critical desire time gap is only 39.04% of PF when velocity = $10m/s$. This indicates that the controller based on PLF can significantly

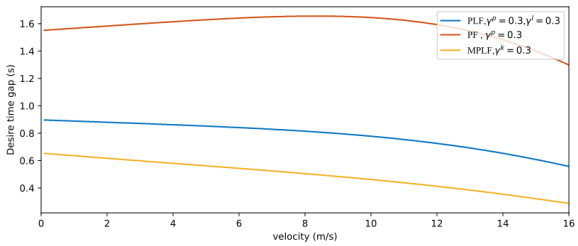

Fig. 3: The phase diagram in the velocity-desire time gap of different IFTs.

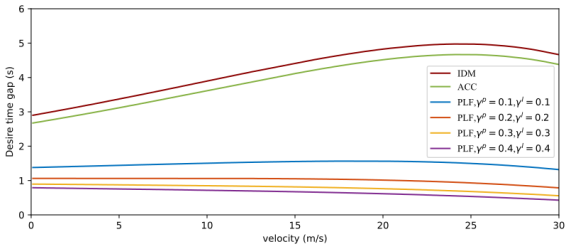

Fig. 4: The phase diagram in the velocity-desire time gap.

improve the stability of traffic flow compared with that on PF on enhancing traffic flow capacity and safety.

As for the margin stable curve of MPLF, it is lower than the curve of PLF, which means that obtaining more information from the preceding vehicles can improve the stability of traffic flow. More communication requirements are needed for MPLF to achieve a smaller desire time gap, but the 34% reduction in the desire time gap will bring a surge in communication requirements that is difficult to achieve. According to corresponding research[31], the failure rate of communication is 16% when the communication frequency is 2 packet/s, and when the communication frequency is 5 packet/s, the failure rate is 38%. This indicates that as the communication demand in the same channel approaches the channel bandwidth, the communication failures will significantly increase. Therefore, the gain of the CACC platoon controller based on MPLF for the desire time gap and its negative impact on communication instability should be considered balanced. In contrast, the communication of PLF can significantly reduce the desire time gap on maintaining communication stability.

2) Margin stable curves of PLF under different parameters: In Section V-A1, PLF is more adaptable in the current technical environment, which leads to another problem: how to set the weighting coefficient of communication gain. For this purpose, the numerical analysis of the different parameter settings is also carried out as follows. Derived from Equation 20, the margin stable curves in the space (velocity-desire time gap) are expressed in Fig. 4.

It can be clearly found in Fig. 4, the margin stable curves of ACC and IDM are of distinct orders of magnitude compared with that of PLF under different parameter settings. For the CACC platoon controller based on PLF, it can be found that the margin stable curves are significantly lower than the ACC curve and are lower as γ_p and γ_l increases, which

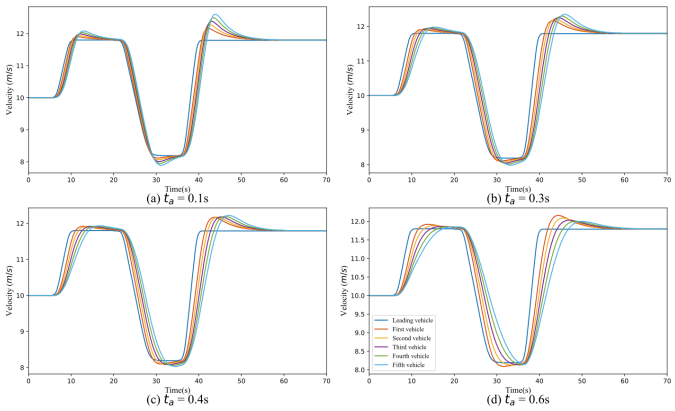

Fig. 5: Time evolutions of the velocity of the simulation platoon for the parameter $t_a = 0.1, 0.3, 0.4, 0.6s$.

means obtaining the information from the preceding vehicle via communication can significantly improve the long-wave stability of traffic flow. From another perspective, the curve of ACC will have a significant peak as the velocity increases, which means that in the 15-30 m/s velocity range, ACC needs a larger time gap to maintain stability, while the CACC platoon based on PLF can also suppress this peak even when γ_p and γ_l are set to 0.1 to ensure that a low time gap can be maintained over the entire velocity range. However, with the γ_p and γ_l increasing, the curves show a trend of getting closer, and the control of the vehicle will tend to follow the control strategy of the preceding vehicle rather than use its own, which means that the controller is more unsafe. For the reasons above, a more significant value of γ_p and γ_l is not necessary for the improvement of string stability, so we choose $\gamma_p = \gamma_l = 0.3$ in the following simulations.

B. Simulation validation

To verify the results of theoretical numerical analysis from the perspective of short-wave stability of traffic flow, the response of the CACC platoon under disturbance is analyzed under open boundary conditions. The simulation scenario is as follows: the simulation platoon includes an MV as the leader vehicle and five CACCs. The CACC following the MV degenerates to ACC, and other vehicles use the general model as the longitudinal control model. At first, all vehicles maintain the same initial velocity of 10m/s and the desire time gap. The form of disturbance is the leader vehicle MV suddenly accelerates to 11.8m/s in 5s and keeps the velocity for 15s. The MV then decelerates back to 8.2m/s and accelerates back to 11.8m/s, while the following vehicles respond to this traffic oscillation scenario. The simulations are carried out by increasing desired time gap t_a from 0.1s to 0.6s. Fig. 5-6 show the time evolutions of the velocity and acceleration of the simulation platoon for the parameter $t_a = 0.1, 0.3, 0.4, 0.6s$.

From Fig. 5-6, we can clearly find that with the increase of the desire time gap t_a, the traffic oscillation generated by the sudden accelerating and decelerating of the leader vehicle MV gradually weakened in the CACC platoon. When $t_a = 0.1, 0.3, 0.4s$, the disturbance increase propagates downstream

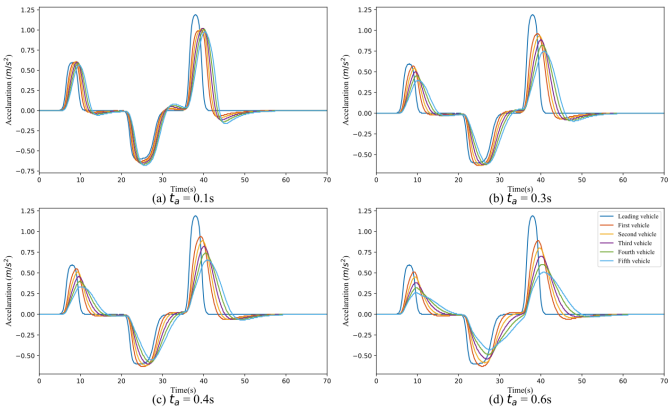

Fig. 6: Time evolutions of the acceleration of the simulation platoon for the parameter $t_a = 0.1, 0.3, 0.4, 0.6s$.

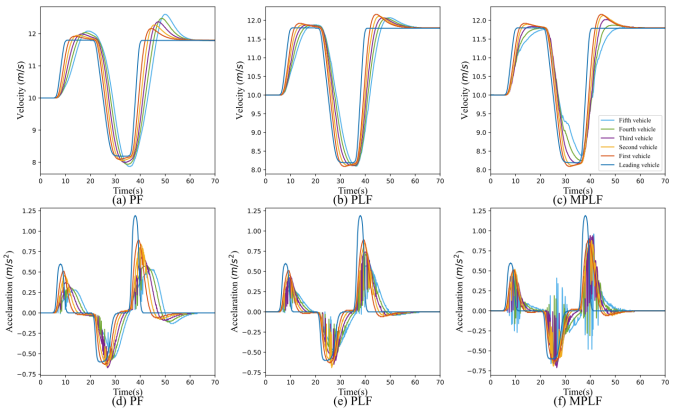

Fig. 7: Time evolutions of the velocity and acceleration of simulation platoon for different IFTs.

with time as shown in Fig. 5-6, which indicates the CACC platoon is string instability, while the disturbance is gradually suppressed as it propagates downstream for $t_a = 0.6s$. The above results show that the theoretical results of linear stability analysis agree with those of the simulation of short-wave stability.

C. Comparisons between different IFTs

In addition to the differences in stability region explored in Section V-A1, the difference of IFTs on robustness, safety, and emission is investigated based on numerical simulation, which is difficult to reflect in the numerical analysis. Many existing studies[32][33] used traffic oscillation scenarios to compare the performance of different vehicle types, which is highly effective. Therefore, we continue to use this method for simulation, and the specific simulation scenario is similar to the one in 5.2.

1) Comparison of robustness: In practical application, packet loss and cyber-attack make the communication environment not absolutely ideal, making it necessary to ensure the robustness of the corresponding IFTs. To verify the robustness of different IFTs, we simulated the CACC platoon equipped with different IFTs in a non-ideal communication environment with 10% packet loss rate and 10Hz communication frequency. IFT parameter settings similar to those in Section V-B are applied in the simulation. The simulation results are shown in Fig. 7.

Packet loss rate appears as a sudden increase or decrease of the acceleration in Fig. 7. Admittedly, poor communication quality can significantly affect the stability of the CACC platoon, especially in continuous packet loss. However, due to high communication frequency, the velocity curves of PF and PLF remain steady. At the same time, few disturbances on accelerations show that platoon controllers designed based on PF and PLF are robust against such communication failures. They can still guarantee smooth driving even under poor communication quality. On the other hand, platoon controllers designed based on MPLF are not robust against such communication failures and will experience significant velocity fluctuations due to its dependence on ideal communication.

TABLE II: Definitions and formulas of indicators used to evaluate safety.

	Definition	Calculation formulas
TTC	Time To Collision	$TTC_t = \frac{x_{L,t} - x_{F,t} - D_L}{v_{F,t} - v_{L,t}}; \forall (v_{F,t} - v_{L,t}) > 0$
MTTC	Maximum Time To Collision	$MTTC_t = \frac{v_{F,t} - v_{L,t} \pm \sqrt{(v_{F,t} - v_{L,t})^2 + 2\Delta a_t (x_{L,t} - x_{F,t} - D_L)}}{\Delta a_t}$
DRAC	Deceleration Rate to Avoid the Crash	$DRAC_{F,t} = \frac{(v_{F,t} - v_{L,t})^2}{2(x_{L,t} - x_{F,t} - D_L)}$

Therefore, PF and PLF are more suitable IFTs in terms of robustness.

2) Comparison of traffic safety: In addition to stability, safety is another essential reference factor for controller design. Several indicators such as TTC, MTTC, PET, DRAC are selected to compare the security performance of platoon controllers based on different IFTs. Table.II provides the definition and calculation formula for each indicator where $x_{L,t}$ and $x_{F,t}$ denotes the positions of the leading vehicle and the following vehicle at time t, respectively; $v_{F,t}$ and $v_{L,t}$ are their velocities at time t; D_L is the length of the leading vehicle; Δa_t is the relative acceleration of conflicting vehicles at time t; $t_{F,t}$ and $t_{L,t}$ are the time of following vehicle arrives and leading vehicle leaves encroachment time. Simulation is implemented based on similar IFT parameter settings in Section V-B. Fig. 8 shows the improvement rate of different IFTs compared with pure MV environment as the baseline on various indicators. It should be noted that the TTC and MTTC are the larger, the safer, while the DRAC is the smaller, the safer. Therefore, the improvement rate mentioned here refers to the growth rate of IFT compared to MV for TTC and MTTC, while it represents the reduction rate for DRAC.

It can be found from Fig. 8 that the application of CACC can significantly improve safety compared to purely manual driving no matter what IFT is used. However, the impact of different IFTs on safety indicators is distinct. For example, adopting PLF or MPLF can cause nearly twice the optimization effect compared to PF, while the difference between PLF and MPLF is tiny. When we pay attention to the difference between PLF and MPLF, we can find that PLF can still maintain a certain advantage compared to MPLF which may b

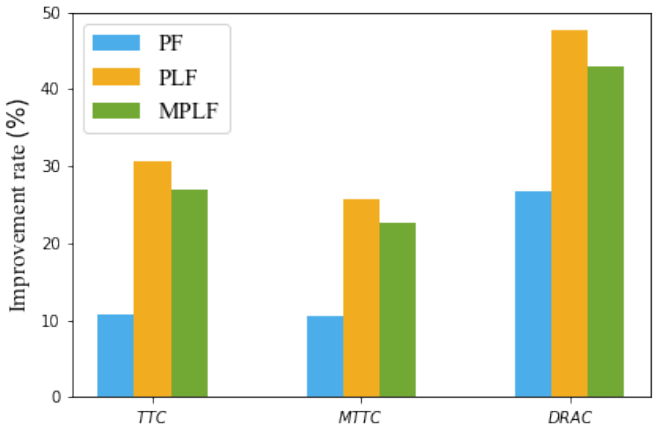

Fig. 8: Improvement rate of indicators among three IFTs against pure MV.

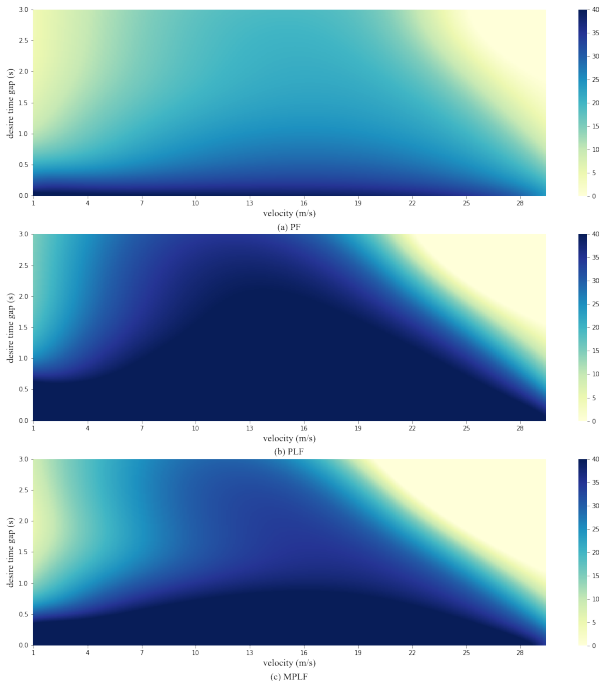

Fig. 9: Improvement rate heatmap of DRAC among three IFTs against pure MV.

e due to the excessive dependence of MPLF on the information from the preceding vehicle. In general, PLF is the best among the three IFTs from the perspective of safety.

A simulation experiment is also carried out with different velocities and desire time gaps to explore the change of the safety indicators in the region of velocity-desire time gap (for simplicity, here, only the DRAC is selected as the comparison indicator). Based on the safety indicator DRAC, optimization heatmaps of three IFTs relative to MV are shown in Fig. 9 where value is expressed as a percentage.

The improvement rate heatmaps of the three IFTs all show a trend that the improvement rate first increases and then decreases as the velocity increases. If PLF is adopted, the improvement rate can reach 40% and above regardless of

TABLE III: Parameters for Emission Model of Petrol Car.

Pollutant		f_1	f_2	f_3	f_4	f_5	f_6
CO_2		5.53e-01	1.61e-01	-2.89e-03	2.66e-01	5.11e-01	1.83e-01
NO_x	$a \geq -0.5$ m/s^2	6.19e-04	8.00e-05	-4.03e-06	-4.13e-04	3.80e-04	1.77e-04
	$a < -0.5$ m/s^2	2.17 e-04	0	0	0	0	0
VOC	$a \geq -0.5$ m/s^2	4.47e-03	7.32e-07	-2.87e-08	-3.41e-06	4.94e-06	1.66e-06
	$a < -0.5$ m/s^2	2.63e-03	0	0	0	0	0
PM		0	1.57e-05	-9.21e-07	0	3.75e-05	1.89e-05

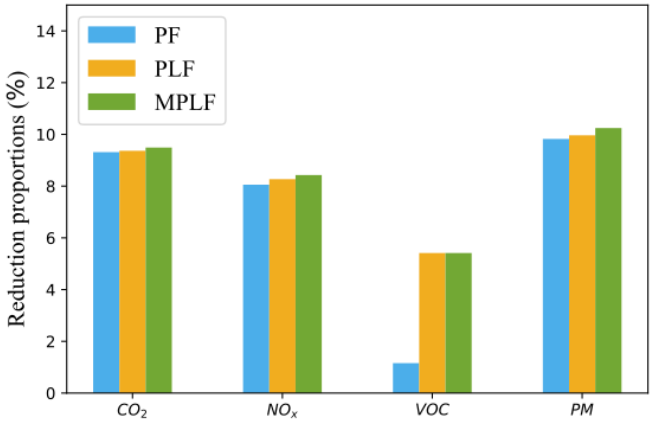

Fig. 10: Pollutants reduction proportion among three IFTs against pure MV.

desired time gap. From the perspective of the desire time gap, it is found that the improvement rate decreases with the increase of the desire time gap. The phenomenon may be explained by that pure MV vehicles tend to be more and more stable with the improvement of the desire time gap. At the same time, CACCs remain stable so that the relative improvement rate is getting smaller and smaller. In addition, when we focus on the differences between the three IFTs, we find that adopting PLF or MPLF can maintain a significant gain compared to PF, and PLF is better than MPLF, which is similar to the conclusion in Fig. 8.

3) Comparison of Eco-driving: With the substantial increase in the number of vehicles, CACCs are also considered a solution, so it is necessary for us to incorporate pollutant emissions into the comparison of different IFTs. Panis et al.[34] established an emission model using a non-linear multivariate regression based on field measurement. The expression for calculation instantaneous traffic emission of a specific vehicle is:

$$E_i(t) = \max\left[0, f_1 + f_2 v_i(t) + f_3 v_i(t)^2 + f_4 a_i(t) + f_5 a_i(t)^2 + f_6 v_i(t) a_i(t)\right], \tag{24}$$

where $E_i(t)$ is the pollutant emission for the vehicle in unit time(g/s); f_1 to f_6 are emission parameters for each type of pollutant; $v_i(t)$ is the velocity of the subject vehicle; and $a_i(t)$ is the acceleration of the subject vehicle. Values of emission parameters are provided in Table.III. The simulation scenario is the same as Section V-B. The results of different IFTs compared with pure MV setting as the baseline are shown in Fig. 10.

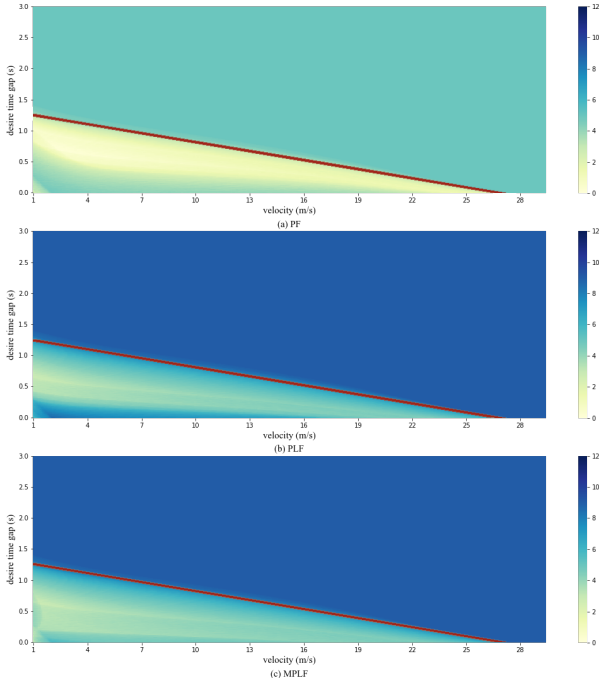

Fig. 11: Reduction proportion heatmap of VOC among three IFTs against pure MV.

From Fig. 10 we can find that the CACCs can effectively reduce the emissions of various pollutants, and the magnitude of emission reduction of different emissions are also different. And different IFTs for the same pollutant can also cause significant differences. PLF and MPLF can cause a nearly 5-fold decrease in VOC relative to PF, while the impact of the three IFTs on reducing CO_2, PM, and NO_x emissions are similar. In addition, the difference of PLF and MPLF on reducing the above four types of emissions are too negligible to distinguish which one is better compared to their volume.

When we look at the difference between different IFTs, we can find from Figure 11 that the reduction proportion improving effect of PLF and MPLF on VOC indicators is indistinguishable, while the impact of PF is less significant than the other two. Moreover, both PLF and MPLF can significantly reduce VOC in the area above the red curve, while the effect of PF in the whole area is less obvious. In addition, an interesting phenomenon can be found from figure 11 that a clear dividing line can be seen on the heatmap of all three IFTs, and the reduction proportion of the upper area of the dividing line can be significantly improved compared to that of the lower area. This phenomenon can be reasonably inferred that this boundary line is the critical line of pure MV performance degradation on VOC. The use of CAV can suppress the appearance of performance degradation, making this red line a crucial line for sudden changes in the reduction proportion. In addition, if we pay attention to the area below the red curve, we can find that the relative relationship between PF and PLF is also consistent with the conclusion in Fig. 11, while the case for PLF and MPLF are slightly different. The reduction proportion heat maps of PLF and MPLF maintain a similar trend overall, but when the desire time gap is in 0-0.3s , and the velocity is in 1-16m/s, it is obvious that PLF is better than MPLF.

VI. Conclusion

This paper designed the platoon controller for CACC strings that formed several platoons due to the limitation of the C-V2X communication range. The model of CACC was firstly proposed based on specific IFTs, and multiple time delays were considered in the design of the general model. To select model parameters, corresponding linear string stability analyses were implemented to obtain the stability condition against a slight disturbance under the open boundary condition. Then, numerical analyses and simulations were carried out to verify the stability region based on the CACC platoon controller from the perspective of long-wave and short-wave stability. Finally, the differences of different IFTs in stability region, robustness, safety, and emission were explored to determine the effect of the CACC platoon controllers based on different IFTs. The following conclusions can be drawn through theoretical analysis:

1) The string stability criterion of the CACC platoon controller indicates that the linear stability is directly related to equilibrium velocity.
2) As the equilibrium velocity increases, the margin stable curve of ACC will have a peak, which indicates that it is difficult for ACC to maintain stability in the velocity range of 15-30 m/s, and the CACC platoon controller based on PLF can directly inhibit the emergence of this peak.
3) CACC platoon controller based on PLF can maintain smaller desire time gap than ACC without losing stability. The control parameters of the controller are as tiny as 0.1 when velocity is set to 14 m/s, indicating a significant traffic capacity and safety gain via communication.
4) With the increase of the control parameters of the CACC platoon controller, the margin stable curve of the desire time gap decreases, but the decline will be smaller and smaller. Therefore, it is not necessary to set control parameters to high values. The optimal control parameter is $\gamma_p = \gamma_l = 0.3$ because the gain of the desire time gap has a diminish marginal effect with further increase of parameters.
5) By comparing the effects of different IFTs from the four perspectives of stability, robustness, safety, and emission, we can find that PLF and MPLF can maintain a significant improvement compared to PF. Still, the difference between the two is not apparent. PLF can keep a slight advantage in robustness and safety, while MPLF is better in stability. However, MPLF requires an ideal communication environment which leads to exponential pressure on communication bandwidth, so that its gain relative to PLF may need to be considered in a balanced manner. In general, PLF is the IFT that is more suitable for the current technical environment and should be used by CACCs.

Acknowledgment

This work was sponsored by the National Science Foundation of China (No. 51878161 and No.52072067) and the China Postdoctoral Science Foundation (No.2020M681466).

References

[1] Z. Wang, Y. Bian, S. E. Shladover, G. Wu, S. E. Li, and M. J. Barth, "A survey on cooperative longitudinal motion control of multiple connected and automated vehicles," *IEEE Intelligent Transportation Systems Magazine*, vol. 12, no. 1, pp. 4–24, 2019.

[2] S. E. Shladover, C. Nowakowski, X.-Y. Lu, and R. Ferlis, "Cooperative adaptive cruise control: Definitions and operating concepts," *Transportation Research Record*, vol. 2489, no. 1, pp. 145–152, 2015.

[3] J. Wang, Y. Zheng, Q. Xu, J. Wang, and K. Li, "Controllability analysis and optimal control of mixed traffic flow with human-driven and autonomous vehicles," *IEEE Transactions on Intelligent Transportation Systems*, 2020.

[4] R. Hall and C. Chin, "Vehicle sorting for platoon formation: Impacts on highway entry and throughput," *Transportation Research Part C: Emerging Technologies*, vol. 13, no. 5-6, pp. 405–420, 2005.

[5] D. N. Yanyan Qin, Hao Wang, "Lwr model for traffic flow mixed with cacc vehicles." *Transportation Science*, 2021.

[6] L. Zhou, T. Ruan, K. Ma, C. Dong, and H. Wang, "Impact of cav platoon management on traffic flow considering degradation of control mode," *Physica A: Statistical Mechanics and its Applications*, p. 126193, 2021.

[7] Y. Zhang, Y. Bai, J. Hu, and M. Wang, "Control design, stability analysis, and traffic flow implications for cooperative adaptive cruise control systems with compensation of communication delay," *Transportation Research Record*, vol. 2674, no. 8, pp. 638–652, 2020.

[8] F. Navas and V. Milanés, "Mixing v2v-and non-v2v-equipped vehicles in car following," *Transportation research part C: emerging technologies*, vol. 108, pp. 167–181, 2019.

[9] C. Wang, S. Gong, A. Zhou, T. Li, and S. Peeta, "Cooperative adaptive cruise control for connected autonomous vehicles by factoring communication-related constraints," *Transportation Research Part C: Emerging Technologies*, vol. 113, pp. 124–145, 2020.

[10] K. Li, Y. Bian, S. E. Li, B. Xu, and J. Wang, "Distributed model predictive control of multi-vehicle systems with switching communication topologies," *Transportation Research Part C: Emerging Technologies*, vol. 118, p. 102717, 2020.

[11] A. Zhou, S. Gong, C. Wang, and S. Peeta, "Smooth-switching control-based cooperative adaptive cruise control by considering dynamic information flow topology," *Transportation Research Record*, vol. 2674, no. 4, pp. 444–458, 2020.

[12] Y. Zheng, S. E. Li, J. Wang, D. Cao, and K. Li, "Stability and scalability of homogeneous vehicular platoon: Study on the influence of information flow topologies," *IEEE Transactions on intelligent transportation systems*, vol. 17, no. 1, pp. 14–26, 2015.

[13] D. Jia, K. Lu, J. Wang, X. Zhang, and X. Shen, "A survey on platoon-based vehicular cyber-physical systems," *IEEE communications surveys & tutorials*, vol. 18, no. 1, pp. 263–284, 2015.

[14] F. Ma, J. Wang, Y. Yang, L. Wu, S. Zhu, S. Y. Gelbal, B. Aksun-Guvenc, and L. Guvenc, "Stability design for the homogeneous platoon with communication time delay," *Automotive Innovation*, vol. 3, pp. 101–110, 2020.

[15] Y. Zheng, S. E. Li, J. Wang, K. Li *et al.*, "Influence of information flow topology on closed-loop stability of vehicle platoon with rigid formation," in *17th International IEEE Conference on Intelligent Transportation Systems (ITSC)*. IEEE, 2014, pp. 2094–2100.

[16] H. Farah and H. N. Koutsopoulos, "Do cooperative systems make drivers' car-following behavior safer?" *Transportation research part C: emerging technologies*, vol. 41, pp. 61–72, 2014.

[17] S. Yu and Z. Shi, "The effects of vehicular gap changes with memory on traffic flow in cooperative adaptive cruise control strategy," *Physica A: Statistical Mechanics and its Applications*, vol. 428, pp. 206–223, 2015.

[18] Z. Li, W. Li, S. Xu, and Y. Qian, "Stability analysis of an extended intelligent driver model and its simulations under open boundary condition," *Physica A: Statistical Mechanics and its Applications*, vol. 419, pp. 526–536, 2015.

[19] P. Fernandes and U. Nunes, "Multiplatooning leaders positioning and cooperative behavior algorithms of communicant automated vehicles for high traffic capacity," *IEEE Transactions on Intelligent Transportation Systems*, vol. 16, no. 3, pp. 1172–1187, 2014.

[20] V. Milanés and S. E. Shladover, "Modeling cooperative and autonomous adaptive cruise control dynamic responses using experimental data," *Transportation Research Part C: Emerging Technologies*, vol. 48, pp. 285–300, 2014.

[21] V. Milanés, S. E. Shladover, J. Spring, C. Nowakowski, H. Kawazoe, and M. Nakamura, "Cooperative adaptive cruise control in real traffic situations," *IEEE Transactions on intelligent transportation systems*, vol. 15, no. 1, pp. 296–305, 2013.

[22] K. C. Dey, L. Yan, X. Wang, Y. Wang, H. Shen, M. Chowdhury, L. Yu, C. Qiu, and V. Soundararaj, "A review of communication, driver characteristics, and controls aspects of cooperative adaptive cruise control (cacc)," *IEEE Transactions on Intelligent Transportation Systems*, vol. 17, no. 2, pp. 491–509, 2015.

[23] D. Ngoduy, "Analytical studies on the instabilities of heterogeneous intelligent traffic flow," *Communications in Nonlinear Science and Numerical Simulation*, vol. 18, no. 10, pp. 2699–2706, 2013.

[24] Z. Yao, T. Xu, Y. Jiang, and R. Hu, "Linear stability analysis of heterogeneous traffic flow considering degra-

dations of connected automated vehicles and reaction time," *Physica A: Statistical Mechanics and its Applications*, vol. 561, p. 125218, 2021.

[25] I. G. Jin and G. Orosz, "Dynamics of connected vehicle systems with delayed acceleration feedback," *Transportation Research Part C: Emerging Technologies*, vol. 46, pp. 46–64, 2014.

[26] J. Sun, Z. Zheng, and J. Sun, "Stability analysis methods and their applicability to car-following models in conventional and connected environments," *Transportation research part B: methodological*, vol. 109, pp. 212–237, 2018.

[27] X. Chang, H. Li, J. Rong, X. Zhao *et al.*, "Analysis on traffic stability and capacity for mixed traffic flow with platoons of intelligent connected vehicles," *Physica A: Statistical Mechanics and its Applications*, vol. 557, p. 124829, 2020.

[28] Y. Li, H. Wang, W. Wang, L. Xing, S. Liu, and X. Wei, "Evaluation of the impacts of cooperative adaptive cruise control on reducing rear-end collision risks on freeways," *Accident Analysis & Prevention*, vol. 98, pp. 87–95, 2017.

[29] A. Kesting, M. Treiber, M. Schönhof, and D. Helbing, "Adaptive cruise control design for active congestion avoidance," *Transportation Research Part C: Emerging Technologies*, vol. 16, no. 6, pp. 668–683, 2008.

[30] A. Kesting, M. Treiber, M. Schönhof, F. Kranke, and D. Helbing, "Jam-avoiding adaptive cruise control (acc) and its impact on traffic dynamics," in *Traffic and Granular Flow'05*. Springer, 2007, pp. 633–643.

[31] K. A. Hafeez, L. Zhao, B. Ma, and J. W. Mark, "Performance analysis and enhancement of the dsrc for vanet's safety applications," *IEEE Transactions on Vehicular Technology*, vol. 62, no. 7, pp. 3069–3083, 2013.

[32] S. Gong, J. Shen, and L. Du, "Constrained optimization and distributed computation based car following control of a connected and autonomous vehicle platoon," *Transportation Research Part B: Methodological*, vol. 94, pp. 314–334, 2016.

[33] X. Li, J. Cui, S. An, and M. Parsafard, "Stop-and-go traffic analysis: Theoretical properties, environmental impacts and oscillation mitigation," *Transportation Research Part B: Methodological*, vol. 70, pp. 319–339, 2014.

[34] L. I. Panis, S. Broekx, and R. Liu, "Modelling instantaneous traffic emission and the influence of traffic speed limits," *Science of the total environment*, vol. 371, no. 1-3, pp. 270–285, 2006.